

## Energy Release by Magnetic Tearing: The Nonlinear Limit\*

Gerard Van Hoven and Mark A. Cross†

Department of Physics, University of California, Irvine, California 92664

(Received 25 August 1972)

The nonlinear limit of the resistive tearing-mode instability is investigated by a time-dependent solution of the Fourier-transformed magnetohydrodynamic equations. The calculation is started with the fastest-growing linear mode and assumes a constant (e.g., turbulent) resistivity. Attainable magnetic Reynolds numbers are limited by the steep spatial gradients developed and by the propagation of Alfvén waves in the system. At the largest values used, 10% of the background energy is released in nonthermal forms. The time and energy scales found are consistent with the results of astrophysical observations and laboratory studies of solar-flare processes.

### I. INTRODUCTION AND BASIC EQUATIONS

We have previously investigated the linear resistive instability in a periodic magnetic field configuration.<sup>1</sup> The calculated growth rate is consistent with the observed time scales in both astrophysical and laboratory situations which are thought to involve a resistive instability. The question remains whether the tearing mode will continue to release energy rapidly when it develops to a nonlinear level. There is also a question of whether this energy will be released in the proper form to account for the observed properties of, for example, solar flares. Here, we will follow the development of the tearing mode, from its known *fastest-growing* linear solution through its fully nonlinear stage, paying particular attention to its total time scale and energy release.

The magnetohydrodynamic equations for our problem are<sup>2</sup>

$$\vec{E} + \vec{v} \times \vec{B}/c = \eta \vec{J}, \quad (1)$$

$$\frac{\partial \vec{B}}{\partial t} = \nabla \times (\vec{v} \times \vec{B}) - \frac{c^2}{4\pi} \nabla \times (\eta \nabla \times \vec{B}), \quad (2)$$

$$\rho \left( \frac{\partial}{\partial t} + \vec{v} \cdot \nabla \right) \vec{v} = -\nabla P + \frac{\vec{J} \times \vec{B}}{c}, \quad (3)$$

$$\frac{\partial \rho}{\partial t} + \nabla \cdot (\rho \vec{v}) = 0, \quad (4)$$

and a derived form of the energy equation

$$\left( \frac{\partial}{\partial t} + \vec{v} \cdot \nabla \right) T = (\gamma - 1) \times \left( \frac{\eta c^2}{16 \pi^2 n k_b} (\nabla \times \vec{B})^2 - T (\nabla \cdot \vec{v}) \right), \quad (5)$$

where the customary symbols have been used. We take the coordinate system of Furth, Killeen, and Rosenbluth,<sup>2</sup> a two-dimensional sheet pinch with  $\partial/\partial z = 0$ . The  $x$  axis is along, and the  $y$  axis is perpendicular to, a neutral line at which a component of  $\vec{B}$  changes sign. Initially, the plasma contains a sheared force-free field described by<sup>1</sup>

$$\vec{B}_0 = \hat{x} B_0 \sin(\pi y/a) - \hat{z} B_0 \cos(\pi y/a) \quad (6)$$

and an equilibrium particle pressure  $\bar{P} = nk_b T$ , which is isotropic. With constant resistivity  $\eta$ , the time development of our background model consists of a slow decay of  $\vec{B}_0$  as the energy in the magnetic field is converted into heat. We have previously found<sup>1</sup> linear solutions for tearing perturbations, with wave numbers along  $x$ , which grow exponentially much more quickly than the initial magnetic field decays.

### II. METHOD OF SOLUTION AND APPROXIMATIONS

Equations (2)–(5) are a coupled system of eight equations for the functions  $\vec{B}$ ,  $\vec{v}$ ,  $T$ , and  $\rho(x, y, t)$ . In principle, these equations could be solved on a computer. We could describe the initial perturbations as functions in a two-dimensional space of discrete points in  $x$  and  $y$  and then follow the time development of  $\vec{B}$ ,  $\vec{v}$ ,  $T$ , and  $\rho$ . This would require a great deal of computer storage and time, and the computer solution of the differential equations may run into a numerical instability associated with the Alfvén-wave propagation discussed in Sec. II C.

We will instead use the results of our previous linear calculations,<sup>1</sup> which involved a spatial Fourier decomposition in the  $y$  direction, as a basis for the nonlinear treatment of this problem. In particular, we will investigate the later time development of the *fastest-growing* small-amplitude excitation.

#### A. Magnitude of Magnetic Reynolds Number

We have shown<sup>1</sup> that the Fourier series (in  $y$ ) of the perturbation functions converges fairly rapidly for moderate magnetic Reynolds number  $S$ , where

$$S = t_r/t_h = 4\pi B_0 a / \eta c^2 (4\pi \rho_0)^{1/2} \quad (7)$$

is the ratio of the resistive decay time to the hydrodynamic (Alfvén-wave) time.<sup>2</sup> This rapid convergence occurs because resistivity tends to destroy

large current densities which produce sharp spatial gradients in the magnetic field, which, in turn, are described by large- $n$  terms in the Fourier expansion. As an example, when  $S=10$ , the fourth nonvanishing  $y$  Fourier coefficient is less than 0.1% of the first. In the explicitly solvable long-wavelength limit (Appendix D of Ref. 2), the reconnection width can be approximated by  $aS^{-1/4}$ , which would indicate that approximately seven Fourier terms in  $y$  should be adequate for  $S=10^3$ , the worst case that we treat. The  $x$  behavior is even more favorable, since nearly all higher-order wave numbers are linearly stable. Magnetic tearing is a long-wavelength instability,<sup>3</sup> and for  $S \leq 10^3$  the third and higher harmonics have temporally decreasing linear amplitudes.

Consequently, if we restrict our attention to cases of moderate resistivity ( $S \leq 10^3$ ), we will need only on the order of  $3 \times 8$  terms to describe a double Fourier series in  $x$ - $y$  space, as opposed to a typical network of  $100 \times 100$  points used to describe the untransformed functions of  $x$  and  $y$ .

In addition to reducing the required computer storage, a lower value of  $S$  increases the size of the time step which may be used to follow the development of the perturbation. Let  $t_h$  be the time scale for propagation of a hydromagnetic disturbance,  $t_r$  the  $e$ -folding time for resistive decay of the initial magnetic field, and  $t_e$  the  $e$ -folding time of the linear mode. We are interested in events on the time scale  $t_e$ , but the computer solution must follow events at  $t_h$ , the fastest of the three time scales. With  $S = t_r/t_h$  and the normalized growth rate<sup>2</sup>  $p = t_r/t_e$ , our linear solution<sup>1</sup> leads to

$$t_e \approx 0.3S^{3/7}t_h \quad (8)$$

as a relation between these time scales. Suppose that  $S \sim 10^{6-8}$ , as is the case for solar flares. Then  $t_e > 100t_h$  and the computer solution must make 100

calculations, at a time step governed by  $t_h$ , to follow the exponential development during the period  $t_e$ . To conserve computer storage and time, we have been restricted to  $S \leq 10^3$  as a practical limit.

### B. Spatial Fourier Decomposition

We have expressed all variables as Fourier series with the following forms:

$$\begin{aligned} v_x(x, y, t) &= \frac{1}{4} \sum_{m,n=-\infty}^{\infty} v_x(m, n, t) \sin \frac{m\pi x}{l} \cos \frac{n\pi y}{a}, \\ v_y(x, y, t) &= \frac{1}{4} \sum_{m,n} v_y(m, n, t) \cos \frac{m\pi x}{l} \sin \frac{n\pi y}{a}, \end{aligned} \quad (9)$$

and so on. In a shorter notation

$$\begin{aligned} B_y, v_x &\sim \sin x \cos y, \\ B_x, v_y &\sim \cos x \sin y, \\ v_z &\sim \sin x \sin y, \\ T, \rho, B_z &\sim \cos x \cos y \end{aligned} \quad (10)$$

indicate the symmetries of the dependent variables of interest.

We will assume constant resistivity  $\eta$ , due, for example, to turbulence,<sup>4</sup> and the condition of incompressibility<sup>2</sup>

$$\nabla \cdot \vec{v} = \frac{m\pi}{l} v_x(m, n, t) + \frac{n\pi}{a} v_y(m, n, t) = 0, \quad (11)$$

which will be justified in Sec. II E. We can then substitute our Fourier series into the  $x$  and  $y$  components of Eq. (2) and the  $z$  component of the curl of Eq. (3) to get

$$\begin{aligned} \frac{\partial B_x(0, i)}{\partial t} &= -\frac{\eta c^2 \pi}{4a^2} i^2 B_x(0, i) \\ &+ \frac{\pi l i^2}{4a^2} \sum_{\substack{m,n=-\infty \\ m \neq 0}}^{\infty} \frac{1}{m} B_y(m, n) v_y(m, i-n), \end{aligned} \quad (12)$$

$$\begin{aligned} \frac{\partial B_y(j, i)}{\partial t} &= -\frac{\eta c^2 \pi}{4l^2} \left( j^2 + i^2 \frac{l^2}{a^2} \right) B_y(j, i) + \frac{\pi j}{4l} \sum_{n=-\infty}^{\infty} B_x(0, i-n) v_y(j, n) \\ &+ \frac{\pi j}{4a} \sum_{\substack{m,n=-\infty \\ m \neq 0, j}}^{\infty} \left( \frac{n}{m} - \frac{j-n}{j-m} \right) v_y(m, n) B_y(j-m, i-n), \end{aligned} \quad (13)$$

and

$$\begin{aligned} \frac{\partial v_y(j, i)}{\partial t} &= \left( \frac{j}{16\rho l(j^2 + i^2 l^2/a^2)} \right) \left[ \sum_{n=-\infty}^{\infty} \left( j^2 + \frac{i(2n-i)l^2}{a^2} \right) B_y(j, n) B_x(0, i-n) \right. \\ &\left. + \frac{l}{a} \sum_{\substack{m,n=-\infty \\ m \neq 0, j}}^{\infty} \left( m^2 + n^2 \frac{l^2}{a^2} \right) \frac{nj-mi}{m(j-m)} [B_y(m, n) B_y(j-m, i-n) - 4\pi\rho v_y(m, n) v_y(j-m, i-n)] \right] \end{aligned} \quad (14)$$

as a nonlinear-mode-coupling description of the system.

### C. Number of Terms in Fourier Series

If the above Fourier series are truncated too quickly in the computer solution of Eqs. (12)–(14), they will not accurately describe the functions we are investigating. On the other hand, we note that hydromagnetic propagation can exist in the model we are studying, so each Fourier coefficient will tend to oscillate at the frequency

$$\omega(m, n) = V_a k = V_a \left( \frac{m^2 \pi^2}{l^2} + \frac{n^2 \pi^2}{a^2} \right)^{1/2} \quad (15)$$

of Alfvén waves. Since this is the fastest time scale in the problem, the larger values of  $m$  and  $n$  will be dominated by Alfvén oscillations rather than by the tearing-mode instability. We must terminate the Fourier series at an  $m$  and  $n$  large enough so that there is little truncation error, yet not so large that Alfvén oscillations dominate. A practical solution to this problem is to first truncate the series at a very small  $m$  and  $n$  and then gradually increase  $m$  and  $n$  until the solution does not change significantly when the maximum  $m$  and  $n$  are changed.

Another important element of this treatment is the use of the fastest-growing linear perturbation<sup>1</sup> as a starting point for the calculation. As an example, when  $S = 10^3$ , the fastest-growing perturbation has normalized wave number<sup>2</sup>  $\alpha \equiv \pi a/l = 0.35\pi$ , according to our linear solution.<sup>1</sup> In addition,  $\alpha \geq \pi$  is known to be linearly stable<sup>3,5</sup>; in verification of this, our computer solution finds that the tearing-mode instability does not cause growth of the Fourier coefficients with  $m \geq 3$  (i. e., wave numbers  $\alpha$  greater than three times the fundamental). Little error is thus caused by truncating the  $x$  Fourier series after  $m = 2$  or 3. This strategy, and that described in Sec. IID, eliminates the problems encountered by Tsuda,<sup>6</sup> who began his calculations with a nonoptimum excitation and found the form of the nonlinear limit to be dependent on the level of the initial perturbation.

The convergence behavior of the Fourier coefficient  $B_y(1, 0)$  is shown in Fig. 1 for truncation of the series after different upper limits  $m$  and  $n$ . The calculations were stopped when most of the initial magnetic field energy had been converted into either heat or the growing perturbation. After the peaks in Fig. 1, all the curves turned downward as resistivity converted  $B_y(1, 0)$  into thermal energy.

All the solutions which follow were found by gradually raising the truncation points of the series until they had little effect on the solution. We never considered terms with  $(m, n)$  larger than  $(4, 10)$ , in the moderate range of  $S$  investigated.

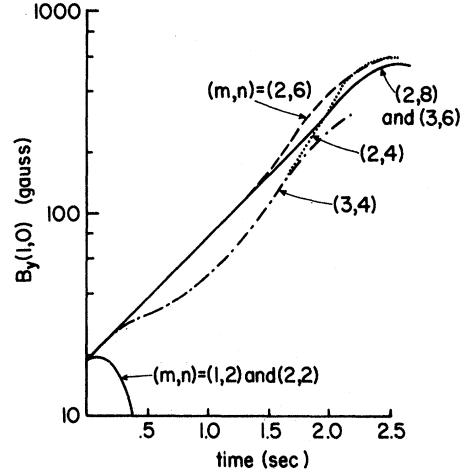


FIG. 1. Convergence of the nonlinear solution as the series truncation limit increases ( $S = 100$ ).

### D. Region of Linearity

The known linear solution is only valid for very small perturbations. It would be inefficient to start with an infinitesimal excitation and find a solution of the full nonlinear equations for 10–20 linear  $e$ -folding times before the perturbation became large enough to show nonlinear effects. We wish to start with the largest perturbation which is still a solution of the linearized equations. We find this largest perturbation by first starting with the “infinitesimal” (fastest-growing) perturbation which has  $B_y(1, 0) \approx 10^{-2} B_x(0, 1)$ , where  $B_x(0, 1)$  describes the initial magnetic field. This solution, with  $S = 10^3$ , is plotted in Fig. 2. Initially,  $B_x(0, 1)$  decays according to

$$\frac{\partial \vec{B}_0}{\partial t} = - \frac{\eta_0 c^2 \pi}{4a^2} \vec{B}_0 = - \frac{\vec{B}_0}{t_r} \quad (16)$$

owing to resistive processes. After the perturbation  $B_y(1, 0)$  exceeds roughly 10–20% of  $B_x(0, 1)$ , we begin to see nonlinear effects, which increase the rate of conversion of energy from the initial magnetic field. We have started all other solutions with a perturbation whose amplitude is roughly  $B_y(1, 0) \sim 0.05 B_x(0, 1)$ .

Figure 2 confirms and extends our earlier linear calculation. The nonlinear solution, in which we permit an arbitrary time dependence, initially exhibits the same exponential linear growth which we calculated earlier, as indicated by the dashed lines in the figure. Consistency in the nonlinear behavior of the instability is shown by the saturation of the perturbation as it approaches the (decaying) equilibrium level.

### E. Compressibility

In Eq. (11) we made the assumption  $\nabla \cdot \vec{v} = 0$ , as suggested by Furth *et al.*<sup>2</sup> This led to the set of

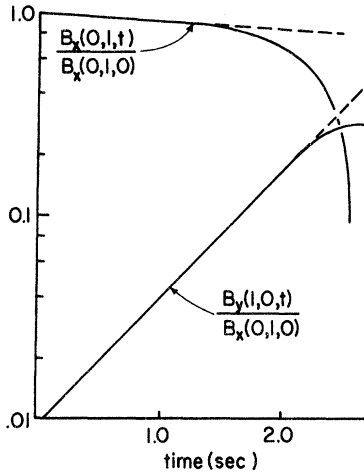


FIG. 2. Region of linearity and approach to saturation when  $S=10^3$ .

equations (12)–(14), in which we needed to solve for three of the unknown functions  $\vec{B}$ ,  $\vec{v}$ ,  $T$ , and  $\rho$ . We now check the validity of this approximation by comparing our incompressible nonlinear solution with a solution that does not assume  $\nabla \cdot \vec{v} = 0$ .

This requires the Fourier transform of all eight of the compressible equations (2)–(5). The eight transformed equations have been detailed elsewhere.<sup>7</sup>

We have obtained a nonlinear compressible solution<sup>7</sup> of the full set of equations for  $S=100$ . The wave number was chosen to be  $\alpha = 0.44\pi$ , which is the fastest-growing wave number for this Reynolds number. (Another dimensionless parameter  $\beta = 8\pi P/B^2$  is needed to specify all the constants appearing in the system of eight equations. The value  $\beta \sim 10^{-6}$ , which is believed to be characteristic of the regions where solar flares originate, was chosen.)

In Fig. 3 we compare portions of the compressible and analogous incompressible nonlinear solutions for  $S=100$ . We find that the assumption  $\nabla \cdot \vec{v} = 0$  has little effect on the linear solution and causes at worst a 10–20% error in the nonlinear solution. The assumption of incompressibility reduces the computer time by a factor of 4 and the storage volume by about a factor of 2. In the work that follows, we have generally assumed  $\nabla \cdot \vec{v} = 0$  and have used Eqs. (12)–(14), except where it was necessary to solve for functions (such as the temperature  $T$ ) which are not included in these equations.

#### F. Physical Parameters

We have left our Eqs. (12)–(14) in cgs units rather than transform them to a system of dimensionless variables. We have used the typical solar-flare parameters<sup>8</sup>  $B_0 = 10^3$  G,  $\rho_0 = 10^{-13}$  g/cm<sup>3</sup>,  $T_0$

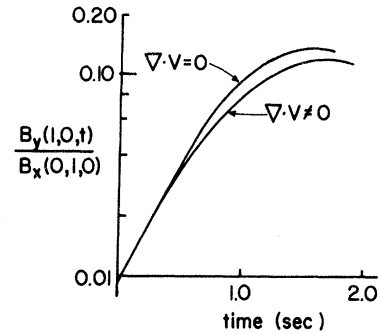


FIG. 3. Effect on the magnetic field of assuming incompressibility, when  $S=100$  and  $\beta=10^{-6}$ .

$= 10^4$  °K,  $a = 10^8$  cm,  $l = 2-3 \times 10^8$  cm, and an artificial resistivity  $\eta$ , which was adjusted to get the value of  $S$  desired.

If the reader is interested in applying the results below to other than the above parameters, we suggest that he first use Eqs. (7) and (16) to obtain  $S$  and  $t_r$ . The linear  $e$ -folding time is then given by

$$t_e \approx 0.3 S^{-4/7} t_r, \quad (17)$$

a restatement of Eq. (8). Finally, the reader will need to calculate the Alfvén speed  $V_a = B_0(4\pi\rho)^{-1/2}$  and the energy in the initial magnetic field.

### III. RESULTS

#### A. Time Scale

In Fig. 4 we plot  $v_y(x=0, y=\frac{1}{2}a)$ , the velocity at which the plasma is moving toward the neutral line. We find that it generally takes about five linear  $e$ -folding times to go from a thermal-level perturbation ( $B_y^2/8\pi \sim nk_b T$ ) to nonlinear saturation under the solar-chromosphere conditions described in Sec. II F. An extrapolation of Fig. 4 shows that,

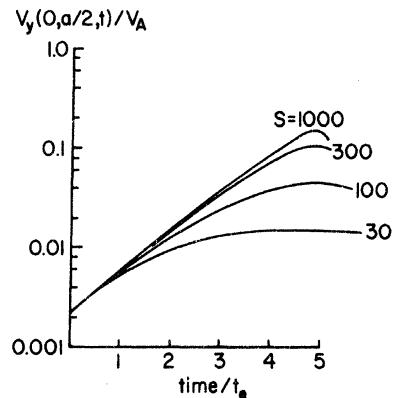


FIG. 4. Convergence of the speed of the fluid entering the region of the tearing mode to more than 15% of the Alfvén speed.

for large  $S$ , the plasma moves toward the neutral line at more than 15% of the Alfvén speed. For the above parameters,  $V_a \sim 0.9 \times 10^9$  cm/sec. If the width of the region in which a solar flare occurs is  $10^9$  cm, then all of the plasma would reach the neutral line in less than 7 sec. This is roughly the observed time for the flash phase of a flare.

In a laboratory plasma<sup>9</sup> with an Alfvén speed of  $10^7$  cm/sec and a scale length of 1 cm, the nonlinear tearing mode could reach its peak release of magnetic field energy in less than  $1 \mu$ sec.

### B. Energy Release

A unit volume for our periodic configuration is  $-\frac{1}{2}l < x < \frac{1}{2}l$ ,  $-\frac{1}{2}a < y < \frac{1}{2}a$ . We can integrate products of the Fourier series over this volume to get the average energy density. For example,

$$\begin{aligned} \langle \frac{1}{2} \rho v_x^2 \rangle &= \frac{1}{V} \iiint \frac{1}{2} \rho v_x^2 d^3V \\ &= \frac{1}{128} \sum_{\substack{ij \\ mn=-\infty}}^{\infty} \rho(m, n) v_x(i+m) v_x(j+n) \quad (18) \end{aligned}$$

and similar expressions occur for the other forms of kinetic, thermal, and magnetic field energy.<sup>7</sup> Our computer solutions conserve total energy to within 0.1%, a good check on their consistency.

Some forms of the energy density averaged over the region of the instability are shown in Fig. 5. The parameters chosen for this solution were taken from the solar-flare conditions described in Sec. II F, with an artificial resistivity  $\eta$ , which was adjusted to make  $S=100$ . The total normalized energy at  $t=0$  does not add up to 1, because half of the energy is initially in the  $z$  component of the magnetic field, which we have not included in the figure. We find that  $\frac{1}{2} \rho v_x^2$  is generally within 20% of  $B_y^2/8\pi$ , indicating that the plasma leaving the instability region moves at its Alfvén speed  $v_x \sim B_y(4\pi\rho)^{-1/2}$ . The temperature quickly rises to

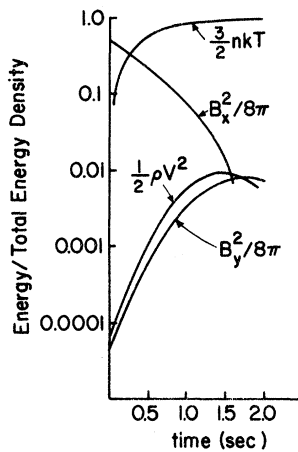


FIG. 5. Various forms of energy in the tearing mode ( $S=100$ ).

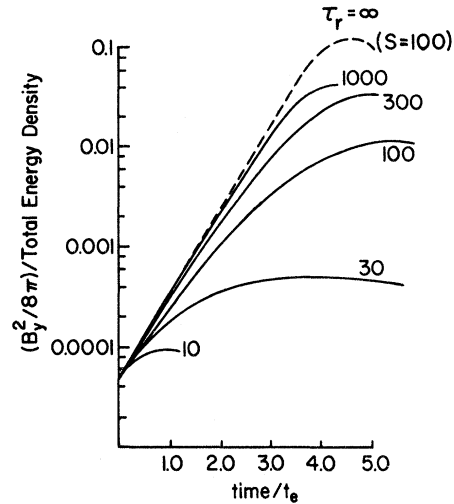


FIG. 6. Energy in the reconnected magnetic field. The dashed  $\tau_r = \infty$  line is obtained by artificially stopping the decay of the background field for  $S=100$ .

more than  $10^9$  °K for the solution in Fig. 5. Most of this heating is due to the resistive decay of the background magnetic field. We suspect that for much larger  $S$  there would still be considerable heating, but we cannot show this due to computer limitations. (This point is discussed in Sec. IV.)

In Figs. 6 and 7 we have plotted the magnetic and kinetic energy as functions of  $S$ . Both components converge to peaks of more than 4% of the initial energy at large Reynolds numbers. We conclude that for  $S \geq 10^3$  the energy in the initial magnetic field is converted into at least 4% fluid kinetic energy and 4% reconnected magnetic field energy, with less than 92% in heat. We have not been able to study directly the nonlinear tearing mode for the large- $S$  values appropriate to astrophysical applications, but we have set limits on the large- $S$  solution by noting the behavior at smaller  $S$ .

We have had to use values of  $S$  which were small enough so that the resistive decay of the initial magnetic field is significant, as in Fig. 5. We can simulate much larger Reynolds numbers by ignoring this resistive decay. We simply drop the decay term, given by Eq. (16), from the right side of Eq. (12). The dashed line in Fig. 6 is the result of a calculation in which the parameters were exactly the same as for the  $S=100$  line, but large Reynolds number was simulated by dropping the resistive-decay term. If this method of investigating  $S \sim \infty$  is valid, then the reconnected magnetic field may have as much as 11% of the initial energy.

The use of a periodic equilibrium has caused our solution to be effectively bounded in  $x$  and  $y$ . The

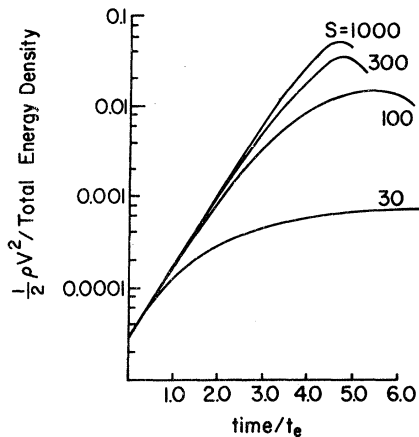


FIG. 7. Fluid kinetic energy in the tearing mode.

nonlinear development of the instability tends to stop when the magnetic pressure  $B_y^2/8\pi$  along the neutral line ( $y=0$ ) is comparable with  $B_x^2/8\pi$  along the lines  $x=\pm l$ , so that the fluid at  $(x=\pm l, y=0)$  is in equilibrium. In a more realistic model of a solar flare, in which the magnetic field configuration is not periodic in  $x$ , the reconnected magnetic field could escape toward  $x=\pm\infty$ , in contrast to our closed periodic "bottled-up" configuration. The plasma flow, in that case, would not develop a back pressure at saturation, as it now does. It would be possible then to convert a higher proportion of the initial energy to fluid flow.

It is of some interest to investigate whether the linear-field topology, or cell structure, persists into the nonlinear regime. We find that our particular solutions, starting from the *fastest-growing* perturbation (which would naturally appear from the ambient noise), retain a single vortex. The higher-order Fourier coefficients are always bounded by the lower-order ones. The one Fourier inversion and field plot made showed one reconnected cell for each reversal and fundamental wavelength. This is an aspect of the work which we intend to pursue further in the future.

Finally, the above results can be applied to the

experimental study of magnetic tearing made by Bratenahl and Yeates.<sup>9</sup> Typical parameters for their work are  $B_0 \sim 10^3$  G,  $\rho \sim 7 \times 10^{-10}$  g/cm<sup>3</sup>,  $a$  (scale width)  $\sim 1$  cm,  $T \sim 2 \times 10^4$  K, and an approximate resistivity  $\eta \sim 2 \times 10^{-15}$  sec. Our Eq. (7) gives  $S \sim 7$ , Eq. (16) gives  $t_r \sim 7 \times 10^{-7}$  sec, and the Alfvén speed is  $V_a \sim 1 \times 10^6$  cm/sec, giving  $t_h = a/V_a \sim 10^{-6}$  sec. Note that the magnetic Reynolds number  $S$  is about  $10^6$  times smaller in this experiment than for a solar flare. Under these laboratory conditions, the tearing mode has a linear  $e$ -folding time, from Eq. (8), of more than  $0.8 \times 10^{-6}$  sec. [This is an underestimate of  $t_e$ , because Eq. (8) is inaccurate when  $S < 10^3$ .<sup>11</sup>] Five times  $t_e$  would indicate a time of about  $4 \times 10^{-6}$  sec for the instability to become fully nonlinear. The observations of Bratenahl and Yeates indicate a time scale of 1–5  $\mu$ sec for magnetic relaxation.

#### IV. CONCLUSIONS

We have followed the tearing mode in time from the linear regime to the large-amplitude limit. We have not assumed a steady-state solution as in previous work on the nonlinear "limit" of the tearing mode.<sup>10</sup>

Our nonlinear solutions show a consistency, always valuable in computer solutions, with the more directly derived behavior of the linearly growing perturbation and the decaying equilibrium field. This initial growth and later saturation (when the perturbation energy approaches the background level) are demonstrated in Figs. 2 and 5.

We have shown that the tearing mode can account for two essential aspects of a solar flare, the time scale and energy conversion. There is also fair agreement with some laboratory observations.

In this work we have assumed that the resistivity is constant. The conventional collisional resistivity is temperature dependent,<sup>11</sup> and would decrease as the plasma is heated by the tearing mode. Preliminary results<sup>12</sup> indicate that, when  $\eta \propto T^{-3/2}$ , the time scale for resistive instability is not greatly changed. This is partially due to the development of resistivity gradients, which then drive the short-wavelength rippling mode.<sup>2</sup>

\*Work supported in part by the National Science Foundation under Grant No. GP 28656.

<sup>1</sup>Present Address: Physics Department, Grambling College, Grambling, La. 71245.

<sup>2</sup>M. A. Cross and G. Van Hoven, *Phys. Rev. A* **4**, 2347 (1971).

<sup>3</sup>H. P. Furth, J. Killeen, and M. N. Rosenbluth, *Phys. Fluids* **6**, 459 (1963).

<sup>4</sup>G. Van Hoven and M. A. Cross, *Phys. Fluids* **14**, 1141 (1971).

<sup>5</sup>B. Coppi and A. Friedland, *Astrophys. J.* **169**, 379 (1971).

<sup>6</sup>E. M. Barston, *Phys. Fluids* **12**, 2162 (1969).

<sup>7</sup>T. Tsuda, Magnetic Field Annihilation with Nonlinear Mode Coupling (Department of Electronics, Kyoto University, Japan,

1968) (unpublished).

<sup>8</sup>M. A. Cross, Ph.D. dissertation (University of California at Irvine, 1972), Physics Dept. Report No. 72-47, 1972 (unpublished).

<sup>9</sup>P. A. Sweet, *Annu. Rev. Astron. Astrophys.* **7**, 149 (1969).

<sup>10</sup>A. Bratenahl and C. M. Yeates, *Phys. Fluids* **13**, 2696 (1970).

<sup>11</sup>H. E. Petschek, in *AAS-NASA Symposium on the Physics of Solar Flares*, edited by W. Hess (U. S. GPO, Washington, D. C., 1964), p. 245.

<sup>12</sup>L. Spitzer, *Physics of Fully Ionized Gases* (Interscience, New York, 1962), p. 136.

<sup>13</sup>M. A. Cross and G. Van Hoven, *Bull. Am. Phys. Soc.* **16**, 1233 (1971).